Orientation and Conformation of Amino Acids in Monolayers Adsorbed at an Oil/Water Interface As Determined by Vibrational Sum-Frequency Spectroscopy

Mark R. Watry and Geraldine L. Richmond*

Department of Chemistry, University of Oregon, Eugene, Oregon 97403

Received: June 21, 2002; In Final Form: September 19, 2002

Vibrational sum-frequency spectroscopy has been employed to acquire vibrational spectra in the C−H stretching region of a variety of monolayers of amino acids adsorbed at the CCl_4/aqueous interface. Analysis of the spectra combined with surface tension measurements has been utilized to determine orientational and conformational characteristics of the L-forms of phenylalanine, lysine, leucine, isoleucine, methionine, tryptophan, threonine, and tyrosine and the aromatic acid L-mandelic acid in monolayers at this interface. Spectra have been acquired under different polarization schemes to allow extraction of orientational and conformational information from spectral fits. The results demonstrate the ability to monitor the orientation of particular side chains in more complex molecules.

Introduction

The behavior of proteins and peptides in biological systems has been and continues to be an important area of chemical research in the quest to understand biological functions at the cellular and molecular level. Many of these functions depend on the effects of interfaces (membrane/water for example) on the conformation of the peptides, proteins, and other macromolecules that play a role in biological processes. While many crystal structures have been determined for various macromolecules, few conformations are known for these molecules in their native environments particularly at interfaces. Buried interfaces are very difficult to study because responses from the bulk generally overwhelm the response from the interface. Vibrational sum-frequency spectroscopy (VSFS) is a relatively recently developed technique that is both interfacially specific and molecularly sensitive.[1,2] Since it is a second-order nonlinear optical process, it is only allowed where there is a lack of inversion symmetry, and since it is a vibrational spectroscopic technique, orientational and conformational information about specific compounds can be obtained. Unfortunately, proteins and peptides are large molecules that can be expected to have highly complex spectra. Therefore, in bringing this new technique to bear on this problem, it is necessary to first study simple systems. Since amino acids are the building blocks for these macromolecules, and since many are surface active in their own right,[3] gaining an understanding of their orientations and conformations and of the observable SF active modes is a valuable endeavor.

In the work described below, the surface tension and VSF spectra of several amino acid monolayers (and one structurally similar compound) were examined after adsorption to the CCl_4/D_2O interface. While not strictly a biological interface, the CCl_4/D_2O interface is a model for the water/hydrophobic interfaces experienced by many biological agents.[4] Spectra were acquired under different polarization schemes to allow the extraction of orientational and conformational information from spectral fits. This information when combined with the data from surface tension measurements provides a molecular perspective of how these amino acids adsorb and orient at an aqueous/hydrophobic interface.

Background

Surface Tension. Surface tension measurements provide information about the surface activity and the number density of adsorbate molecules at interfaces.[5] Surface pressure measurements yield isotherms of surface pressure as a function of bulk solution concentration, and these isotherms provide the limiting (maximum) surface excess concentration of molecules at the interface through use of the Gibbs equation:[6]

$$\Gamma_i = \frac{1}{nRT}\left(\frac{\partial \pi}{\partial \ln(a_i)}\right)_T$$

where Γ_i is the surface excess concentration at maximum surface coverage, π is the interfacial pressure in mN/m, n is the number of species in excess at the interface, and a_i is the activity. Γ_i is obtained from a least-squares fit to the linear portion of a plot of π vs $\ln(a_i)$. When the bulk concentration is significant, as is the case here, the contribution from the bulk to the surface concentration must be taken into account since the Gibbs equation gives only the surface excess concentration. In the studies described below, $n = 1$ for the zwitterionic amino acids because there is one new species introduced into the interfacial system, and $n = 2$ for the dissociated L-mandelic acid because one new species is introduced into the interfacial system and the hydrogen ion concentration is significantly changed in the interfacial system.[7] Although it has recently been suggested that these values may not always be correct,[8] in simple systems like the ones studied here they provide the most accurate representation of the data. In the analysis described below, concentrations are used in place of activities even though solution concentrations are high because activity coefficients for amino acids do not vary significantly from unity in aqueous solution even near solution saturation.[9−12]

Spectroscopy. VSFS was first treated theoretically by Bloembergen and Pershan in 1962[13] and was first demonstrated experimentally by Shen et al. in 1987.[2] It is a second-order nonlinear optical technique that is interface specific and sensitive to the molecular species present at the interface. In the experiment, a laser beam with a fixed visible frequency is overlapped spatially and temporally with a tunable infrared

10.1021/jp021469e CCC: $22.00
Published on Web 11/08/2002

beam. This induces a nonlinear polarization in the medium under study, and this nonlinear polarization generates a coherent beam at the sum of the two incident frequencies. The intensity of the generated sum-frequency beam is then measured and recorded as a function of the incident IR frequency. The sum-frequency intensity depends on the square of the second-order polarization in the following manner:

$$I(\omega_{sfg}) \propto |P^{(2)}|^2 \propto |\tilde{f}_{sfg} f_{vis} f_{IR} \chi^{(2)} : E_{vis} E_{IR}|^2 \quad (1)$$

where $\tilde{f}_{sfg}$, f_{vis}, and f_{IR} are the Fresnel coefficients for each of the fields and $\chi^{(2)}$ is the macroscopic second-order susceptibility of the medium. The Fresnel coefficients account for the geometry of the experiment and the effect it has on the effective electric fields at the interface, their polarizations, and their propagation directions. The nonlinear susceptibility is the macroscopic response of the medium to the incident electric fields. Sum-frequency conversion efficiency is enhanced when the infrared beam is in resonance with a molecular vibration. The resonant contributions to the nonlinear susceptibility can be separated from the nonresonant contribution as follows:

$$\chi^{(2)} = \chi^{(2)}_{NR} + \sum_{\nu} \chi^{(2)}_{R}(\nu) \quad (2)$$

where the sum is over all vibrational modes of all molecular species in the medium. The resonant macroscopic susceptibility of a vibrational mode is related to the molecular susceptibility for that mode β_ν as follows:

$$\chi^{(2)}_{R}(\nu) = \frac{N}{\epsilon_0} \langle \beta_\nu \rangle \quad (3)$$

where the brackets indicate an orientational average and N is the number of molecules contributing to the sum-frequency response. Under the dipole approximation, the molecular hyperpolarizability β_ν has the following form, which is derived from perturbation theory:

$$\beta_{lmn,\nu} \propto \frac{\langle g|\alpha_{lm}|\nu\rangle\langle\nu|\mu_n|g\rangle}{\omega_{IR} - \omega_\nu + i\Gamma_\nu} \quad (4)$$

where the numerator is the Raman transition probability multiplied by the IR transition probability, ω_{IR} is the frequency of the incident IR electric field, and Γ_ν is the natural line width of the transition. Since the hyperpolarizability vanishes if either the Raman transition probability or the IR transition probability is zero, VSFS is forbidden in media possessing an inversion center. (Conversely, it is naturally allowed at an interface.) When the laser is tuned over a vibrational resonance of a molecule, the denominator in eq 4 becomes very small, resulting in a large enhancement in the hyperpolarizability and subsequently the sum-frequency intensity. After convolving eq 4 with a Gaussian to account for inhomogeneous broadening, eqs 2−4 can be combined to obtain the following expression:[14]

$$\chi^{(2)} = \chi^{(2)}_{NR} e^{i\phi} + \sum_{\nu} \int_{-\infty}^{\infty} \frac{A_\nu e^{i\varphi_\nu} e^{-[\omega_L - \omega_\nu/\Gamma_\nu]^2}}{\omega_{IR} - \omega_L + i\Gamma_L} \, d\omega_L \quad (5)$$

where the complex exponentials represent the relative phases between the various contributions, A_ν is the numerator from eq 4, and the integral is over Lorentzian lines (centered at ω_L with a width Γ_L) having a Gaussian distribution. The spectra are fit using this expression. In the experiments described below, the Lorentzian widths are set to 2 cm^{-1}, and Γ_ν is allowed to vary since we cannot separate the two contributions to the line width.[15] In addition, some of the spectra do not show evidence of a nonresonant contribution, and in those cases the amplitude is fixed at zero.

The macroscopic nonlinear susceptibility is a 27-element tensor that has only four independent nonzero elements in a system with $C_{\infty v}$ symmetry. Utilizing the convention with p-polarized light polarized in the plane of incidence and s-polarized light polarized perpendicular to the plane of incidence, the ssp polarization combination (where the shorthand notation ssp corresponds to the polarizations of the sum-frequency, visible, and IR, respectively) probes only the element χ_{yyz}, which is sensitive to IR transition dipoles that have a component normal to the interface. The sps polarization combination probes only χ_{yzy}, which is sensitive to IR transitions that have a component in the plane of the interface.

Experimental Considerations

Sample Preparation. The L-forms of the amino acids isoleucine (99%), leucine (99%), lysine monohydrate (97%), methionine (99%), phenylalanine (99%), and tryptophan (99%) were purchased from Avocado Research Chemicals Ltd. through Alfa Aesar and used as received. L-Mandelic acid (99+%) was also purchased from Avocado and used as received. All of the above were tested for purity using surface tension. D_2O (99.9%) was purchased from Cambridge Isotopes Labs and used as received. HPLC grade carbon tetrachloride (99.9+%) was purchased from Sigma-Aldrich and tested for purity in the C−H stretching region by FTIR. Reagent grade sodium phosphate (monobasic) was purchased from Mallinckrodt and dried before use in preparing the buffer.

Interfaces were prepared by placing 25.0 mL of the D_2O solution of the compound of interest (buffered to pD 7.0; 100 mM in total phosphate) over 38 mL of CCl_4 in a custom Teflon cell fitted with CaF_2 windows. Interfaces were allowed to equilibrate for 2 h, which was ample time considering that surface tension reached equilibrium much sooner and that spectra taken 1 h apart after this time were identical.

Prior to their use, all sample cell parts and any glassware used in sample preparation were cleaned using NoChromix reagent followed by rinsing with copious amounts of Nanopure water and allowed to dry.

Surface Tension. All surface tension measurements were made using the Wilhelmy plate method.[16,17] A platinum plate cleaned with NoChromix reagent in sulfuric acid, rinsed in HPLC water, and then flamed until glowing was used for the measurements. This cleaning procedure was repeated before each measurement. Individual amino acid solutions (in 100 mM phosphate buffer pH 7.0) were made by dilution from a concentrated stock solution, and 25 mL of aqueous solution was carefully poured or pipetted over 20 mL of CCl_4 that had already been pipetted into a crystallization dish 60 mm in diameter. The plate was lowered to a consistent depth, and the surface pressure was recorded after the interface reached equilibrium.

Spectroscopic Measurements. The laser and tunable IR source used in these experiments has been described in detail elsewhere[18] so only a brief overview will be given here. The 1064 nm output of a Nd:YAG laser operating at 20 Hz with a 3.5 ns pulse duration is spit into two beams. The first is frequency-doubled to 532 nm using a doubling crystal, and the power of this beam is maintained at a constant but adjustable value. The second is used to generate tunable IR (2600−4000 cm^{-1}) in an OPO−OPA assembly producing 1−4 mJ/pulse with

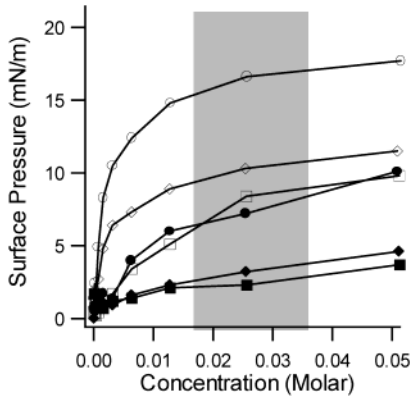

Figure 1. Surface pressure isotherms of L-phenylalanine (○), L-lysine monohydrate (◇), L-leucine (●), L-isoleucine (□), L-mandelic acid (◆), and L-methionine (■) in pH 7.0 buffer at the CCl_4/H_2O interface at 20 °C. The shaded area indicates the bulk concentration range in which monolayer coverage is attained.

a bandwidth of 1 cm^{-1}. The IR is focused at the interface and overlapped spatially and temporally with the ~1 mm diameter visible beam. A total internal reflection geometry is utilized in which the visible beam is incident upon the interface near its critical angle, and the generated sum-frequency light is collected near its critical angle. This geometry can result in an enhancement in the generated sum-frequency intensity by more than 2 orders of magnitude.[19−21] The input and output polarizations can be selected, and the sum-frequency signal is separated physically from the reflected beams using apertures and optically through the use of appropriate filters. The resulting signal is collected by focusing the beam into a PMT and through the use of gated electronics. A power spectrum of the tunable IR is collected simultaneously with the VSFS spectrum, and the spectra are corrected for IR power and the wavelength dependence of the transmission of the collection optics. All spectra described below were acquired by averaging 200 shots per data point, and data were taken every wavenumber over the spectral region. The ssp and sps spectra were acquired consecutively on the same sample without changing the angles of the incoming laser beams or the angle of the PMT. All spectra were corrected for the wavelength dependence of the collection optics, the IR laser power, and Fresnel factors so that direct comparisons may be made between intensities in the ssp and sps spectra.

Results and Discussion

Surface Tension. Most of the essential amino acids are soluble in excess of 0.1 M in water and insoluble in organic solvents. In solution they are zwitterionic. Their surface activity is dependent on the hydrophobicity of the side chain balanced with the degree of aqueous solvation of the acid and amine groups. Figure 1 shows the surface pressure isotherms for L-phenylalanine (○), L-lysine monohydrate (◇), L-leucine (●), L-isoleucine (□), L-mandelic acid (◆), and L-methionine (■) in pH 7.0 buffer at the CCl_4/H_2O interface (top to bottom, respectively). Each of these compounds is moderately surface active, reaching monolayer coverage at bulk concentrations between 18 and 35 mM with reductions in surface tension of 3−17 mN/m. One might expect the surface pressure isotherm to level off or become a line with zero slope once monolayer coverage has been achieved; however, the chemical potential of the solution continues to change as the concentration of the surfactant increases, resulting in a continued change in the surface pressure. The monolayers are not tightly packed with individual molecules occupying 100−200 $Å^2$ at maximum surface coverage (Table 1). The amino acids with the bulkiest hydrophobic side chains (phenylalanine, leucine, and isoleucine) form the most tightly packed monolayers whereas the less bulky methionine and the polar lysine form less tightly packed monolayers. Mandelic acid, an aromatic acid with a structure similar to phenylalanine, is very soluble in aqueous solution and forms the most expanded monolayers. It is interesting to note that leucine and isoleucine have essentially identical surface pressure isotherms (within experimental error) but significantly different solubilities. This suggests that the hydrophobicity of the side chains is equivalent at this interface and that the headgroup area limits the spacing between molecules at monolayer coverage. In all cases the amino acid headgroup area is much greater than the side chain cross-sectional area limiting the side chain−side chain interactions that are a common feature of surfactant monolayers.

TABLE 1: Molecular Areas and Surface Pressures for Monolayers of Amino Acids in 100 mM Phosphate Buffer (pD 7.0) at the CCl_4/D_2O Interface

compound	minimum molecular area ($Å^2$ per molecule, ±10%)	surf. press. at monolayer coverage (mN/m, ± 1)
L-phenylalanine	103	17
L-lysine monohydrate	153	11
L-leucine	118	8
L-isoleucine	114	8
L-mandelic acid	210	4
L-methionine	162	3
L-threonine	*a*	*a*
L-tyrosine	*b*	*b*

[a] Not surface active. [b] Not determined due to low solubility.

In these studies, pH 7.0 phosphate buffer was employed for three reasons. First, this pH is biologically relevant. Second, the amino acids are zwitterions at this pH which simplifies the surface tension analysis considerably. Third, the phosphate is not surface active. The surface tension of the CCl_4/buffer interface is nearly identical to that of the neat CCl_4/H_2O interface. The buffer was observed to have an effect on the solubility of the amino acids with a low solubility. The solubilities were reduced, but the ability to measure a surface pressure isotherm was not affected. This reduction in solubility is probably present for the highly soluble amino acids but was not perceptible in the experiments performed, and it was not investigated.

Spectroscopy. Because vibrational sum-frequency spectroscopy is a coherent process, accurate interpretation of SF spectra requires fitting the data with attention given to the symmetry, orientation, and relative phase of the contributing vibrational transition moments. In an incoherent linear spectroscopy like IR absorption, the spectrum is deconvolved into vibrational peaks whose intensities add together to return the full spectrum. In contrast, the spectral intensity in VSFS is not a simple sum of individual vibrational intensities, and this is clearly shown in eqs 1 and 5. Assignments for methyl and methylene groups have been made in previous VSFS studies[14,15,22] based on vibrational studies of long alkyl chains,[23,24] and those assignments are used here wherever warranted without further reference.

Figure 2a shows ssp (○) and sps (●) spectra of the CCl_4/D_2O interface saturated with L-isoleucine. Isoleucine exhibits four peaks in the ssp spectrum of a complete monolayer. In Figure 2b, the ssp spectrum has been deconvolved to show the contribution of each vibrational mode to the spectrum. The two prominent peaks are the methyl symmetric stretch at 2880 cm^{-1} and the methyl Fermi resonance at 2933 cm^{-1}, and the two weak

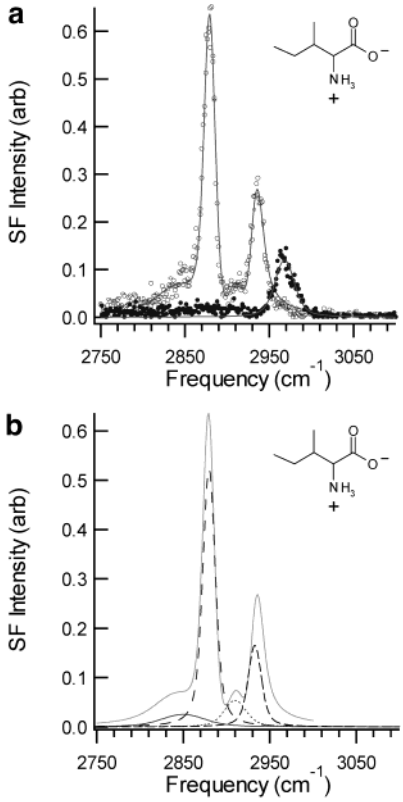

Figure 2. (a) SF spectra of 0.1 M L-isoleucine in pH 7.0 phosphate buffer. The polarization schemes are ssp (○) and sps (●), and the solid lines are fits to the data. (b) The fit to the ssp spectrum along with the deconvoluted peaks.

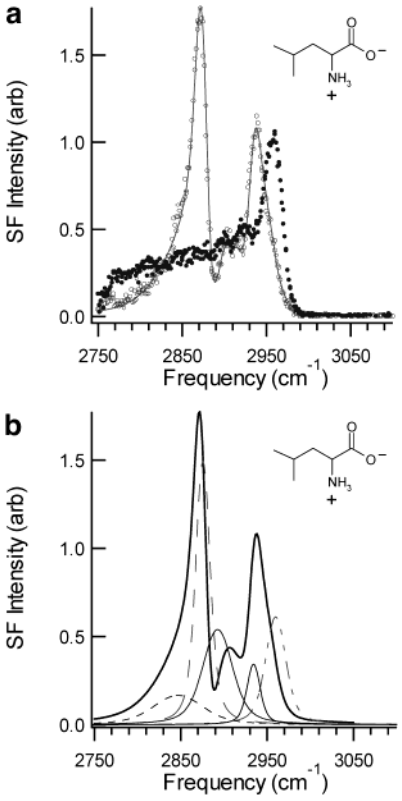

Figure 3. (a) SF spectra of 0.1 M L-leucine in pH 7.0 phosphate buffer. The polarization schemes are ssp (○) and sps (●), and the solid line is a fit to the ssp data. (b) The fit to the ssp spectrum along with the deconvoluted peaks.

peaks are the methylene symmetric stretch at 2850 cm^{-1} and methylene Fermi resonance at 2910 cm^{-1}. There is only one resolvable peak in the sps spectrum, the methyl asymmetric stretch at 2968 cm^{-1}. Since the IR transition moments for the methyl symmetric and asymmetric stretches are perpendicular to each other, and the transition moment for the methyl symmetric stretch is along the symmetry axis of the methyl group, both spectra indicate that the methyl groups in isoleucine are oriented primarily along the normal to the interface. Although it is difficult to imagine that the symmetry axis of both methyl groups could simultaneously lie along the surface normal, the time-averaged orientations of the methyl groups may.

L-leucine is an isomer of L-isoleucine having both methyl groups on the same carbon atom rather than on adjacent carbon atoms. Figure 3 shows ssp and sps spectra of the CCl_4/D_2O interface saturated with L-leucine. Leucine exhibits five peaks in the ssp spectrum of a complete monolayer as determined from spectral fits. These are the methylene symmetric stretch at 2847 cm^{-1}, the methyl symmetric stretch at 2876 cm^{-1}, the methylene Fermi resonance at 2893 cm^{-1}, the methyl Fermi resonance at 2934 cm^{-1}, and the methyl asymmetric stretch at 2960 cm^{-1}. There is intensity from several modes in the sps spectrum, but the only resolvable feature is the methyl asymmetric stretch at ~2960 cm^{-1}. The sps spectrum cannot be unambiguously fit given the number of unconstrained parameters in the fit. On the basis of the significant intensity in both the methyl symmetric stretch and the methyl asymmetric stretch in the ssp spectrum, it is clear that the methyl groups do not lie along the surface normal or in the plane of the interface but have some orientation in between.

Spectra of a monolayer of L-methionine are presented in Figure 4. This amino acid has an alkyl side chain like the

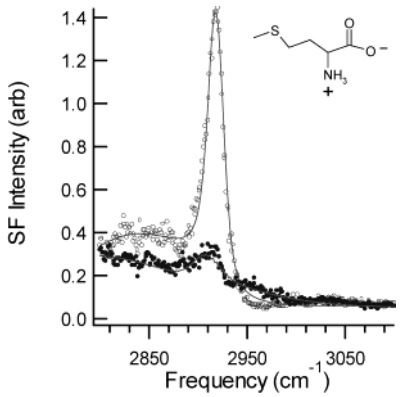

Figure 4. SF spectra of 0.1 M L-methionine in pH 7.0 phosphate buffer. The polarization schemes are ssp (○) and sps (●), and the solid lines are fits to the data.

previous two amino acids; however, it is classified as hydrophilic due to the sulfur atom embedded in the chain with its attendant lone electron pairs. The hydrophilic nature of the side chain compared to isoleucine and leucine is evident in the surface tension data. Methionine reduces the surface tension very little (3 mN/m) at monolayer coverage with a large area occupied per molecule. The ssp spectrum of methionine shows three peaks. The prominent peak at 2920 cm^{-1} is assigned to the symmetric stretch of a methyl group adjacent to a sulfur atom.[25] The broad feature around 2850 cm^{-1} represents methylene symmetric and asymmetric stretches from different parts of the molecule, the methylene adjacent to a sulfur atom, the methylene between the two carbon atoms, and their associated methylene Fermi resonances. A nonresonant contribution to the nonlinear susceptibility is evidenced by the intensity above 3000 cm^{-1} and by the dip in intensity around 2960 cm^{-1} and is included

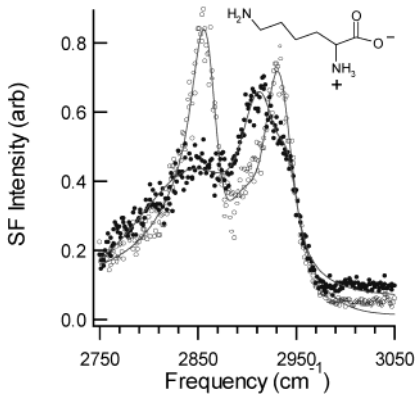

Figure 5. SF spectra of 0.1 M L-lysine in pH 7.0 phosphate buffer. The polarization schemes are ssp (○) and sps (●), and the solid lines are fits to the data.

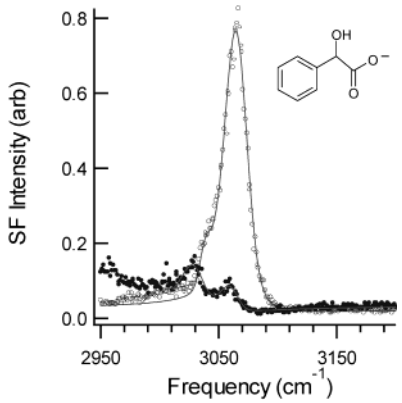

Figure 6. SF spectra of 0.1 M L-mandelic acid in pH 7.0 phosphate buffer. The polarization schemes are ssp (○) and sps (●), and the solid lines are fits to the data.

in the spectral fits. It is interesting to note that the nonresonant contribution appears only in the spectra of the compounds having an electron-rich, or polarizable, group in the side chain. These groups include the sulfur in methionine, amine in lysine, and the aromatic rings in phenylalanine, mandelic acid, and tryptophan. The sps spectrum shows a small contribution from the methyl symmetric stretch, indicating that the methyl group is not oriented entirely along the interface normal. Assuming a delta function orientational distribution, the angle between the symmetry axis of the methyl group and the surface normal is estimated to be 10° with an uncertainty of ±10°.

L-lysine is another amino acid with a hydrophilic alkyl side chain; however, the chain is terminated with an amine. The hydrophilic nature of the side group affects the surface activity and monolayer formation as evidenced in the surface tension data. The area per molecule at monolayer coverage is significantly higher for lysine compared to the hydrophobic amino acids, commensurate with the hydrophilic nature of the side chains whereas the surface tension reduction is significant (and similar to isoleucine and leucine) possibly due to hydrogen bonding of surface water with the alkylamine. The ssp and sps spectra (Figure 5) show peaks at 2860, 2912, and 2935 cm^{-1} assigned to the methylene symmetric stretch, methylene Fermi resonance, and methylene asymmetric stretch of a methylene adjacent to an amine,[25] respectively. Methylene groups in an all-trans conformation have local centers of inversion at the midpoint of the C−C bonds and subsequently would be sum-frequency inactive. Therefore, the significant intensity in all three modes under both polarizations indicates that the methylene chain contains several gauche defects, which is consistent with the hydrophilic nature of the side group and the large area per molecule that prevents interactions between the chains. Additionally, the amines at the end of the chains may be attracted to each other or the aqueous phase, further accentuating these gauche conformations.

Although L-mandelic acid is not an amino acid, it is included in this study to aid in the assignment of the phenylalanine spectra since it has a structure similar to that of phenylalanine. Mandelic acid is very soluble in aqueous solution and exhibits surface properties that are very different from phenylalanine. It is weakly surface active, giving rise to a surface tension reduction of only 4 mN/m at monolayer coverage with a molecular area of 210 Å^2, twice that of phenylalanine. The hydrophobic group on mandelic acid is smaller than that in phenylalanine and contains a hydroxide group that can hydrogen bond to water. In both the ssp and the sps spectra (Figure 6), there are two peaks at 3037 and 3066 cm^{-1}. These peaks correspond to aromatic C−H stretches of monosubstituted benzenes, particularly ν_{7b} and ν_2, respectively.[26] A nonresonant contribution is included in the fits to account for the intensity between 3100 and 3200 cm^{-1}. Aromatic C−H stretching modes have been seen previously in VSFS experiments in this laboratory[27] and by Bain et al.[28,29] The IR transition moment for ν_2 lies on the symmetry axis of the ring, and the moment for ν_{7b} lies off axis. The relative intensities in the ν_2 mode between the ssp and sps spectrum suggest that the ring does not stand vertically at the interface. The phase relationships between the peaks in the spectra make it appear to the eye that the ν_2 peak is much more intense in the ssp spectrum than in the sps spectrum and that the ring is aligned primarily along the surface normal. However, the fitted peaks indicate that this is not the case and that the symmetry axis of the ring is tilted at 24 ± 10° from the normal (assuming a delta function distribution). Given the close proximity between the hydroxide group and the aromatic ring, it is likely that the ring is partially solvated in the aqueous phase resulting in the tilt of the ring. The intensities of ν_{7b} in the spectra are in agreement with this orientation.

The ssp spectrum of L-phenylalanine (Figure 7a) is very similar to that of mandelic acid with peaks at 3037 and 3064 cm^{-1}. The spectra of both compounds were fit as a set considering the similarities of the spectra so the same assignments are made here. There is, however, an additional peak in the sps spectrum of L-phenylalanine at 3090 cm^{-1} that is consistent with Raman and IR assignments of ν_{20a} in monosubstituted benzenes.[26] The peak assignments were made on the basis of not only peak positions but also the relative IR and Raman intensities of the vibrational modes. ν_2 is generally strong to very strong, ν_{7b} is generally medium to strong, and ν_{20a} is generally weak to medium in IR and Raman strength. Again, casual inspection of the spectra suggests that the ν_2 mode is much more intense (~8 times as intense) in the ssp spectrum than in the sps spectrum. However, the fitted peaks indicate a ratio of ~3, resulting in a tilt angle of the symmetry axis of the ring of 18 ± 5° from the surface normal under the assumtion of a delta function distribution of tilt angles.

Figure 7b,c shows how deceptive simple inspection of the spectra can be particularly when there is a contribution from the nonresonant term. Figure 7b shows the fit to the ssp spectrum along with the individual vibrational and nonresonant contributions to the spectrum. In this spectrum, both vibrational peaks are enhanced by the nonresonant contribution, particularly the peak at 3037 cm^{-1}. Figure 7c shows the sps spectral fit along with the individual contributions to the spectrum, showing enhancement and diminishment of various peaks depending on

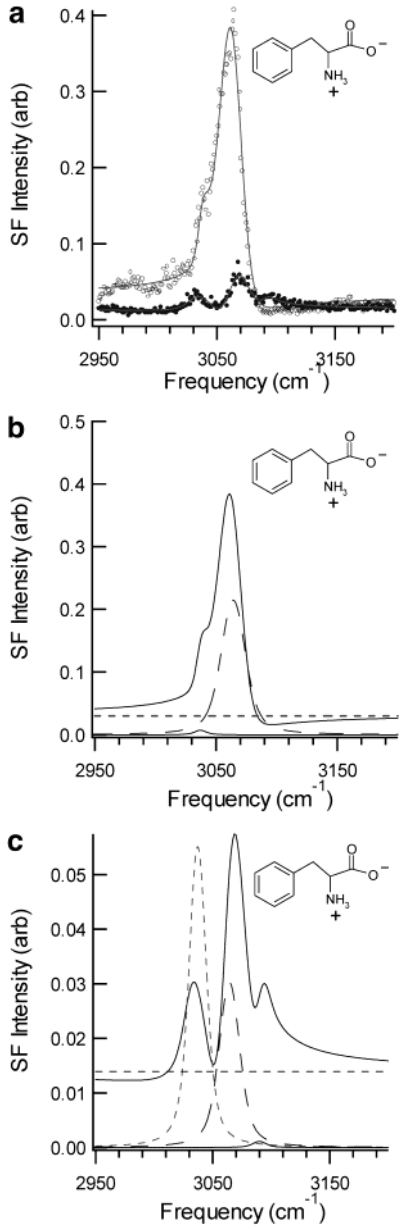

Figure 7. (a) SF spectra of 0.1 M L-methionine in pH 7.0 phosphate buffer. The polarization schemes are ssp (○) and sps (●), and the solid lines are fits to the data. (b) The fit to the ssp spectrum along with the deconvoluted peaks. (c) The fit to the sps spectrum along with the deconvoluted peaks.

the phase relationships between each of the individual peaks and the nonresonant part of the susceptibility.

Since fluorescence from tryptophan provides information about the local environment of the indole side chain, it is commonly used as a fluorescent probe to study the local environment in peptides and proteins.[30−32] It would be experimentally useful if tryptophan could play a similar role in VSFS studies of peptides and proteins at liquid surfaces. An ssp spectrum of an interface prepared from a nearly saturated solution of L-tryptophan is presented in Figure 8. Tryptophan has a low solubility in aqueous solution (less than 50 mM) that is even lower in buffered solution. The monolayer does not exhibit very much SF activity in the ssp spectrum with only one peak observed in the aromatic C−H stretching region at 3058 cm^{-1}. This feature may be composed of more than one peak, but the data do not indicate the necessity of including additional peaks. The sps spectrum does not show any vibrational signal; however, there is a nonresonant contribution

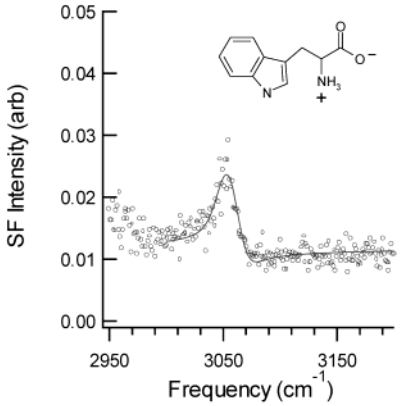

Figure 8. SF spectrum of 0.027 M L-tryptophan in pH 7.0 phosphate buffer. The polarization scheme is ssp (○), and the solid line is the fit to the data.

present in these spectra. The low intensity in the ssp spectrum seen here may not preclude the use of tryptophan as a probe in VSFS. Resonant enhancement of the SF signal with the visible laser beam tuned to an electronic transition of the indole group is likely to greatly improve vibrational sensitivity.

Two additional amino acids were examined in this study as indicated in Table 1. They are L-threonine and L-tyrosine, both having hydrophilic side chains. Threonine is very soluble in aqueous solution but did not have a significant effect on surface tension. (The effect was very similar to that of NaCl.) Threonine also exhibited no intensity in the C−H stretching region in VSF spectra of a 0.1 M solution in buffer. Tyrosine is structurally very similar to phenylalanine. The only difference is an hydroxyl group in the para position on the aromatic ring, However, it has a very low solubility in aqueous solution (<0.3 mM), and VSF spectra showed no intensity in the C−H stretching region for a nearly saturated solution in buffer.

Conclusions

These experiments show VSFS to be a useful tool in the study of amino acid side chains at a liquid surface. The spectra of a variety of amino acid side chains, both hydrophobic and hydrophilic, are accessible in the C−H stretching region. VSFS and surface tension measurements were employed to investigate the orientation and conformation of the L-amino acids phenylalanine, lysine, leucine, isoleucine, methionine, tryptophan, threonine, and tyrosine and the aromatic acid L-mandelic acid at the CCl_4/aqueous interface. Each compound except for threonine and tyrosine exhibited significant SF intensity in the C−H stretching region, and phenylalanine and mandelic acid expressed several aromatic C−H stretching vibrations. Each of the amino acids forms loosely packed monolayers (>100 Å^2 per molecule), and those amino acids with hydrophobic side chains pack more tightly in a complete monolayer than those with hydrophilic side chains.

The spectra of two of the amino acids, methionine and phenylalanine, show unique vibrational features. In methionine, the methyl symmetric stretch is shifted from ∼2878 to 2920 cm^{-1}, and in phenylalanine there are three SF-active aromatic ring vibrations. Spectra of the compounds with polarizable groups in their side chains exhibit nonresonant contributions whereas previous studies have found liquid surfaces to generate a negligible nonresonant response.[33] The results of these experiments are particularly encouraging in that they suggest that the application of VSFS to the study of orientation and conformation of amino acid residues in more complex biological systems will be a fruitful endeavor.

Acknowledgment. The authors are grateful for the financial support provided by the National Science Foundation, CHE 9725751, and by the Office of Naval Research for instrumentation.

References and Notes

(1) Zhu, X. D.; Suhr, H.; Shen, Y. R. *Phys. Rev. B* **1987**, *35*, 3047−3050.

(2) Guyot-Sionnest, P.; Hunt, J. H.; Shen, Y. R. *Phys. Rev. Lett.* **1987**, *59*, 1597−1600.

(3) Bull, H. B.; Breese, K. *Arch. Biochem. Biophys.* **1974**, *161*, 665−70.

(4) Tanford, C. *The Hydrophobic Effect: Formation of Micelles and Biological Membranes*; Wiley-Interscience Publications: New York, 1973.

(5) Rosen, M. J. *Surfactants and Interfacial Phenomena*; John Wiley and Sons: New York, 1978.

(6) Gibbs, J. W. *The Collected Works of J. Willard Gibbs*; Yale University Press: New Haven, CT, 1948; Vol. 1.

(7) Joos, P. *Dynamic Surface Phenomena*; VSP BV: Utrecht, The Netherlands, 1999.

(8) Bae, S.; Haage, K.; Wantke, K.; Motschmann, H. *J. Phys. Chem. B* **1999**, *103*, 1045−1050.

(9) Cohn, E. J.; Edsall, J. T. In *Interactions Between Organic Solvents and Dipolar Ions Estimated from Solubility Ratios*; Cohn, E. J., Edsall, J. T., Eds.; Reinhold Publishing Corp.: New York, 1943; pp 196−216.

(10) Kuramochi, H.; Noritomi, H.; Hoshino, D.; Nagahama, K. *J. Chem. Eng. Data* **1997**, *42*, 470−474.

(11) Smith, P. K.; Smith, E. R. B. *J. Biol. Chem.* **1940**, *132*, 47−56.

(12) Smith, P. K.; Smith, E. R. B. *J. Biol. Chem.* **1940**, *132*, 57−64.

(13) Bloembergen, N.; Pershan, P. S. *Phys. Rev.* **1962**, *128*, 606−622.

(14) Bain, C. D.; Davies, P. B.; Ong, T. H.; Ward, R. N.; Brown, M. A. *Langmuir* **1991**, *7*, 1563−1566.

(15) Goates, S. R.; Schofield, D. A.; Bain, C. D. *Langmuir* **1999**, *15*, 1400−1409.

(16) Rame, E. *J. Colloid Interface Sci.* **1997**, *185*, 245−251.

(17) Davies, J. T.; Rideal, E. K. *Interfacial Phenomena*, 2nd ed.; Academic Press: New York, 1963.

(18) Scatena, L. F.; Richmond, G. L. *J. Phys. Chem. B* **2001**, *105*, 11240−11250.

(19) Bloembergen, N.; Simmon, H. J.; Lee, C. H. *Phys. Rev.* **1969**, *181*, 1261−1271.

(20) Conboy, J. C.; Daschbach, J. L.; Richmond, G. L. *J. Phys. Chem.* **1994**, *98*, 9688−9692.

(21) Dick, B.; Gierulsky, A.; Marowsky, G. *Appl. Phys. B: Laser Opt.* **1985**, *38*, 107−116.

(22) Ward, R. N.; Duffy, D. C.; Davies, P. B.; Bain, C. N. *J. Phys. Chem.* **1994**, *98*, 8536−8542.

(23) Snyder, R. G.; Hsu, S. L.; Krimm, S. *Spectrochim. Acta* **1978**, *34A*, 395−406.

(24) Snyder, R. G.; Strauss, H. L.; Elliger, C. A. *J. Phys. Chem.* **1982**, *86*, 5145−5150.

(25) Socrates, G. *Infrared and Raman Characteristic Group Frequencies: Tables and Charts*, 3rd ed.; John Wiley and Sons Ltd.: West Sussex, 2001.

(26) Varsanyi, G. *Assignments for Vibrational Spectra of Seven Hundred Benzene Derivatives*; John Wiley and Sons: New York, 1974; Vol. 1.

(27) Watry, M.; Richmond, G. L. *J. Am. Chem. Soc.* **2000**, *122*, 875−883.

(28) Bain, C. D.; Bell, G. R.; Duffey, D. C.; Ward, R. N. *Mol. Phys.* **1996**, *88*, 269−280.

(29) Bain, C. D.; Li, Z. X.; Bell, G. R. *J. Phys. Chem. B* **1998**, *102*, 9461−9472.

(30) Clayton, A. H. A.; Sawyer, W. H. *Eur. Biophys. J.* **2002**, *31*, 9−13.

(31) Engelborghs, Y. *Spectrochim. Acta, Part A* **2001**, *57*, 2255−2270.

(32) Lakowicz, J. R. *Photochem. Photobiol.* **2000**, *72*, 421−437.

(33) Miranda, P. B.; Shen, Y. R. *J. Phys. Chem. B* **1999**, *103*, 3292−3307.